

## Melting of Alloy Clusters: Effects of Aluminum Doping on Gallium Cluster Melting

Colleen M. Neal, Anne K. Starace, and Martin F. Jarrold\*

Department of Chemistry, Indiana University, 800 East Kirkwood Avenue, Bloomington, Indiana 47405

Received: December 16, 2006; In Final Form: May 28, 2007

Calorimetry measurements have been performed as a function of temperature for size-selected  $\text{Ga}_{n-1}\text{Al}^+$  clusters with  $n = 17, 19, 20, 30\text{--}33, 43, 46,$  and  $47$ . Heat capacities determined from these measurements are compared with previous results for pure  $\text{Ga}_n^+$  clusters. Melting transitions are identified from peaks in the heat capacities. Substituting an aluminum atom appears to have only a small effect on the melting behavior. For clusters that show melting transitions, the melting temperatures and latent heats for the  $\text{Ga}_{n-1}\text{Al}^+$  clusters are similar to those for the  $\text{Ga}_n^+$  analogs. For  $\text{Ga}_n^+$  clusters that do not show first-order melting transitions ( $n = 17, 19,$  and  $30$ ) the  $\text{Ga}_{n-1}\text{Al}^+$  analogs also lack peaks in their heat capacities. The results suggest that the aluminum atom is not localized to a specific site in the solid-like  $\text{Ga}_{n-1}\text{Al}^+$  clusters.

### Introduction

If two or more metals are mixed, the resulting alloy often exhibits properties that are different from those of the pure constituents. The alloy may be a homogeneous solid solution, a heterogeneous mixture of two or more components, or a chemical compound. Miscible metals form substitutional solid solutions. An important requirement for solid solutions is that the diameters of the constituent atoms should not be substantially different from each other (i.e., they should differ by  $<15\%$ ). Substitution by different-sized atoms leads to compressive or tensile forces on the neighboring atoms which is one factor that contributes to the favorable engineering properties of alloys. Most alloys melt over a range of temperatures where solid and liquid components (with different compositions) coexist. However, for most binary alloys there is a ratio (called the eutectic) that has a single melting point which is usually substantially below that of the pure constituents.

Properties change as dimensions are reduced into the nanometer regime. In the cluster size regime ( $<10^3$  atoms) the properties of an alloy are expected to be sensitive to both the total number of atoms and the composition. In the past few years there has been growing interest in mixed-metal or alloy clusters containing tens or hundreds of atoms.<sup>1–16</sup> In this size regime, adding or subtracting even a single atom may make a huge difference to the properties. It is possible that there are special sizes and compositions that have unique properties, for example, enhanced catalytic activity. Alloy clusters may also provide building blocks for new materials. If the constituent atoms have similar sizes and chemical properties, then the alloy clusters probably consist of a series of isomers with the same topological structure but with different permutations of the atoms between the sites (homotops<sup>11</sup>). On the other hand, if the two atoms are different, they may segregate. Whether or not segregation occurs depends on the strengths of the interactions between the similar and dissimilar atoms. A size mismatch may help to drive segregation. If segregation occurs, the components may adopt a side-by-side or core–shell arrangement, depending on the surface energies. The component with the lower surface energy will tend to segregate to the surface. Segregation may stabilize

a different structural form. For example, in a cluster following icosahedral packing, the internal bonds are shorter than the surface bonds, and so this geometry becomes increasingly strained as it grows larger. A core–shell arrangement with smaller metal atoms inside a shell of larger metal atoms relieves the strain and stabilizes geometries based on icosahedra.<sup>11,13,14</sup>

In this paper we report the first experimental studies of the melting transitions of alloy clusters. It is only recently that experimental studies of the melting of size-selected clusters have become possible. The pioneering work of Haberland and collaborators focused on the melting of sodium clusters.<sup>17–23</sup> We have now performed studies for tin,<sup>24,25</sup> gallium,<sup>26–29</sup> sodium chloride,<sup>30</sup> and aluminum clusters.<sup>31,32</sup> Small particles have melting points that are depressed relative to the bulk value due to the increase in the surface to volume ratio.<sup>33</sup> However, in the small size limit, some clusters (for example, tin and gallium) remain solid above the bulk melting point. In most of the studies referenced above, the melting transitions were monitored using calorimetry. Here the heat capacity is determined as a function of temperature, and the melting transition is indicated by a spike in the heat capacity due to the latent heat. Gallium clusters with up to 55 atoms show large variations in their melting temperatures. The melting temperatures of  $\text{Ga}_{34}^+$  and  $\text{Ga}_{47}^+$  differ by more than 300 K.<sup>27</sup> There are also large size-dependent variations in the latent heats, with some clusters apparently melting without a significant peak in their heat capacities,<sup>28</sup> in what appears to be the finite size analog of a second-order phase transition. This behavior has been attributed to the clusters having disordered ground states.<sup>29,34,35</sup> Here we investigate phase transitions in  $\text{Ga}_{n-1}\text{Al}^+$  clusters where an aluminum atom has been substituted for a gallium atom. In the macroscopic world, the gallium and aluminum alloy has a eutectic at 2.1 atom % aluminum that melts at 299.8 K (slightly below the melting point of bulk gallium which is at 302.9 K). Sputtering experiments suggest that the aluminum segregates away from the surface layer in the liquid eutectic.<sup>36</sup>

Calorimetry measurements were performed by determining the cluster's dissociation threshold as a function of its initial temperature. As the initial temperature is raised, the amount of energy that must be added to reach the dissociation threshold decreases because of the cluster's internal energy. The change

\* Corresponding author. E-mail: mfj@indiana.edu.

in the energy required to reach the dissociation threshold with respect to the temperature provides a measure of the heat capacity of the cluster. A melting transition involving a latent heat leads to a peak in the heat capacity. We take the center of the peak to be the melting temperature, and the area under the peak is a measure of the latent heat.

### Experimental Methods

The experimental methods and the assumptions employed to interpret the results have recently been described in depth,<sup>32</sup> so only a brief overview is given here. The  $\text{Ga}_{n-1}\text{Al}^+$  clusters were generated by pulsed laser ablation of a liquid aluminum/gallium alloy. The alloy was made by mixing aluminum filings into a liquid gallium sample. Aluminum/gallium ratios of around 2 atom % were employed. Gallium has several stable isotopes which causes the gallium cluster peaks in the mass spectrum to become very broad, and so a small aluminum/gallium ratio was used to keep the mass spectrum of the alloy clusters as simple as possible. With the aluminum/gallium ratios used here, pure gallium clusters are the most abundant species in the mass spectrum, and the  $\text{Ga}_{n-1}\text{Al}^+$  clusters are around one-third as abundant. The alloy sample is heated in the source to around 40 °C to keep it liquid. A liquid sample is used here because the surface regeneration that occurs with a liquid prevents the formation of a pit where the laser strikes the surface. The long- and short-term signal stability with the liquid metal target is much better than for a source with a rotating rod or disc.<sup>37</sup>

After formation, the buffer gas flow carries the clusters into a 10 cm long temperature-controlled extension which can be varied between 123 and 1273 K. Measurements have shown that the clusters reach thermal equilibrium in this region.<sup>26</sup> After passing through the extension, some of the cluster ions exit and are focused into a quadrupole mass spectrometer. The size-selected clusters that are transmitted through the quadrupole are focused into a collision cell containing 1 torr of helium. As the ions enter the collision cell they undergo a series of collisions with the buffer gas, each one converting a small fraction of the ion's kinetic energy into internal energy of the cluster and kinetic energy of the helium collision partner. If the initial kinetic energy is large enough some of the ions dissociate. The product ions and unfragmented parents are carried across the collision cell by a weak electric field. At the other side of the collision cell some of the ions exit through a small aperture and are focused into a second quadrupole mass spectrometer, where they are mass analyzed and then detected.

### Results

The  $\text{Ga}_{n-1}\text{Al}^+$  clusters fragment by sequential loss of gallium atoms. Mass spectra are recorded, and the fraction of the  $\text{Ga}_{n-1}\text{Al}^+$  clusters that dissociate is determined. Measurements are performed as a function of the ion's initial translational energy, and the translational energy for 50% dissociation (TE50%D) is determined from a linear regression analysis of measurements performed at typically six different initial kinetic energies. The temperature of the extension is then adjusted, and the measurements are repeated. The TE50%D values decrease as the temperature is raised because the internal energy increases. At the melting transition there should be a sharp drop in the TE50%D values due to the latent heat. The derivative of TE50%D with respect to temperature is proportional to the heat capacity. The proportionality constant is related to the fraction of the ion's kinetic energy that is converted into internal energy. This fraction is estimated using a simple impulsive collision model.<sup>38,39</sup> The fraction depends on the mass of the collision

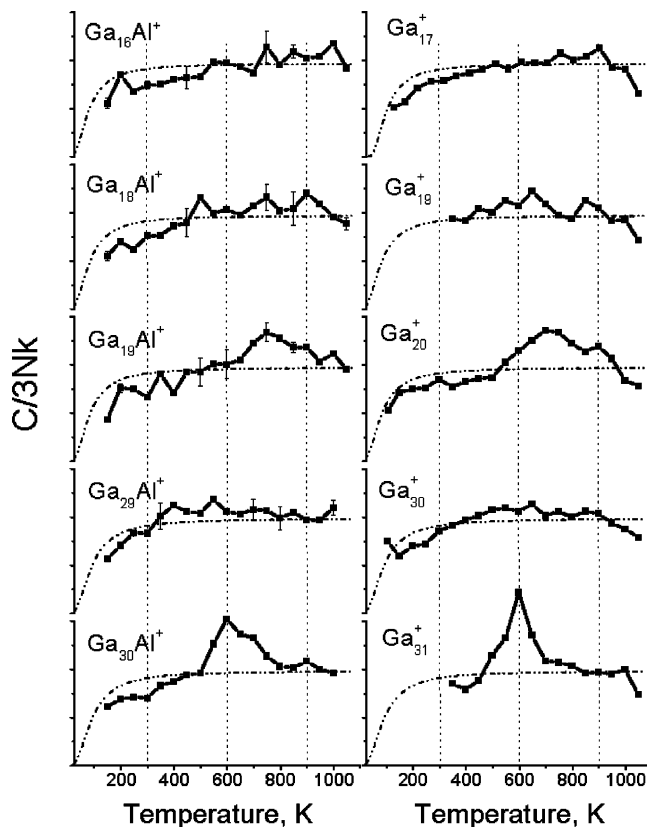


**Figure 1.** Plots of the heat capacities against temperature for pure  $\text{Ga}_n^+$  clusters (from refs 26–29) and for their  $\text{Ga}_{n-1}\text{Al}^+$  analogs for  $n = 17, 19, 20, 30,$  and  $31$ . The heat capacities are plotted in terms of the classical value,  $C/3Nk$ , where  $3N = 3n - 6 + 3/2$ . The dashed-dotted lines in the figures show heat capacities calculated using a modified Debye model that incorporates finite size effects (ref 40). Error bars show representative uncertainties ( $\pm 1$  standard deviation) on the measurements for the  $\text{Ga}_{n-1}\text{Al}^+$  clusters.

gas, and it is small for a light collision gas because of the restrictions placed on energy transfer by momentum conservation. We choose helium as a collision gas in this work because it is a poor collision partner (the fraction of the ion's kinetic energy that is converted into internal energy is a few percent), and thus small changes in the ion's internal energy lead to large changes in the TE50%D values. This amplification is a critical feature of the method.

Figures 1 and 2 show plots of the heat capacities against temperature for pure  $\text{Ga}_n^+$  clusters<sup>26–29</sup> and their  $\text{Ga}_{n-1}\text{Al}^+$  analogs for  $n = 17, 19, 20, 30–33, 43, 46,$  and  $47$ . The heat capacities are plotted in terms of the classical value,  $C/3Nk$ , where  $3N = 3n - 6 + 3/2$  (there are  $3n - 6$  vibrational modes, and the  $3/2$  results from the rotational contribution). The dashed-dotted lines in the figures show heat capacities calculated using a modified Debye model that incorporates finite size effects;<sup>40</sup> the rotational contribution is treated classically. The results shown in Figures 1 and 2 are the results of multiple independent measurements. Error bars show typical uncertainties in the measurements based on  $\pm 1$  standard deviation.

For clusters with  $n = 17$  and  $19$ , both the  $\text{Ga}_n^+$  clusters and the  $\text{Ga}_{n-1}\text{Al}^+$  analogs do not show significant peaks in their heat capacities. For the 20-atom clusters there is a broad peak in the heat capacity for the pure gallium cluster centered at around 700–750 K. The peak for the  $\text{Ga}_{19}\text{Al}^+$  analog is slightly smaller and narrower than that for the pure cluster, and the center is shifted to higher temperature by around 40–50 K.

Pure gallium clusters with 30, 31, 32, and 33 atoms show substantial size-dependent differences in their melting behavior.

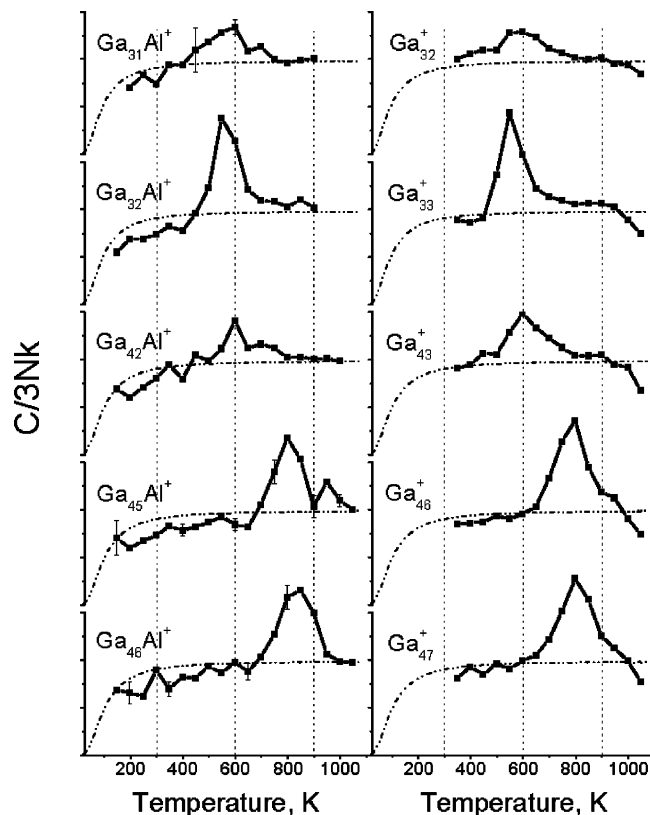


**Figure 2.** Plots of the heat capacities against temperature for pure  $\text{Ga}_n^+$  clusters (from refs 26–29) and for their  $\text{Ga}_{n-1}\text{Al}^+$  analogs for  $n = 32, 33, 43, 46,$  and  $47$ . The heat capacities are plotted in terms of the classical value,  $C/3Nk$ , where  $3N = 3n - 6 + 3/2$ . The dashed-dotted lines in the figures show heat capacities calculated using a modified Debye model that incorporates finite size effects (ref 40). Error bars show representative uncertainties ( $\pm 1$  standard deviation) on the measurements for the  $\text{Ga}_{n-1}\text{Al}^+$  clusters.

The heat capacities for  $\text{Ga}_{30}^+$  do not show a significant peak, whereas those for the  $\text{Ga}_{31}^+$  and  $\text{Ga}_{33}^+$  show substantial peaks, and  $\text{Ga}_{32}^+$  shows a small peak. The results for  $\text{Ga}_{29}\text{Al}^+$  are identical to those for  $\text{Ga}_{30}^+$ ; there is no significant peak in the heat capacities for either of these clusters. For  $\text{Ga}_{30}\text{Al}^+$  there is a substantial peak in the heat capacity. The peak is slightly broader than for  $\text{Ga}_{31}^+$  and appears to be shifted to a slightly higher temperature. The shift, which is around 15–25 K, is difficult to see without overlaying the heat capacity plots.  $\text{Ga}_{31}\text{Al}^+$  and  $\text{Ga}_{32}^+$  both show relatively small peaks in their heat capacities.  $\text{Ga}_{32}\text{Al}^+$  shows a large peak in its heat capacity that is almost identical in position and size to that measured for  $\text{Ga}_{33}^+$ .

There is a substantial shift in the melting temperature between  $\text{Ga}_{43}^+$  and  $\text{Ga}_{46}^+$  that is reproduced in the  $\text{Ga}_{n-1}\text{Al}^+$  analogs. The heat capacities of  $\text{Ga}_{42}\text{Al}^+$  show a small peak at around 600 K that appears to be slightly smaller and narrower than that observed for  $\text{Ga}_{43}^+$ . In contrast, the peaks in the heat capacities for  $\text{Ga}_{46}^+$  and  $\text{Ga}_{45}\text{Al}^+$  are both centered at around 800 K. The peak for  $\text{Ga}_{45}\text{Al}^+$  is shifted to a slightly (20–30 K) higher temperature than the peak for  $\text{Ga}_{46}^+$ . The  $\text{Ga}_{46}^+$  and  $\text{Ga}_{45}\text{Al}^+$  peaks are similar in size. The dip in the  $\text{Ga}_{45}\text{Al}^+$  peak at 900 K is a reproducible feature that does not have an analog in the results for  $\text{Ga}_{46}^+$ . The peaks for  $\text{Ga}_{47}^+$  and  $\text{Ga}_{46}\text{Al}^+$  are also centered at around 800 K. And again the peak for the aluminum-containing cluster appears to be shifted to a slightly (35–45 K) higher temperature than the peak for the pure gallium analog.

Figure 3 shows a plot of the melting temperatures and latent heats determined from the heat capacity plots for the pure gallium clusters (filled points) and the clusters with an aluminum

atom (open points). The melting temperatures are taken from the center of the peak in the heat capacity plots. The peaks are broad, leading to an uncertainty in the melting temperature of around 25–50 K (depending on how sharp the peak is). However, the shifts in the melting temperatures between the  $\text{Ga}_n^+$  and  $\text{Ga}_{n-1}\text{Al}^+$  clusters, which can be obtained by overlaying the heat capacity plots, are more reliable. The uncertainty in the shifts is estimated to be 10–20 K (depending on how sharp the peaks are). We do not expect a significant systematic error between the measurements of the  $\text{Ga}_n^+$  and  $\text{Ga}_{n-1}\text{Al}^+$  clusters. The latent heats are determined from the area under the peak in the heat capacity plots. The uncertainty in the latent heats is estimated to be 10–20  $\text{kJ mol}^{-1}$ . The differences between the latent heats for the  $\text{Ga}_n^+$  and  $\text{Ga}_{n-1}\text{Al}^+$  clusters are more reliable. As shown in Figure 3, the latent heats for the  $\text{Ga}_{n-1}\text{Al}^+$  clusters are in most cases similar to or slightly less than the values for the corresponding  $\text{Ga}_n^+$  clusters.

## Discussion

There are a lot of similarities between the heat capacities for the pure gallium clusters and those measured for the aluminum-containing analogs. The variations in the size of the peaks in the heat capacities are largely reproduced. This is best illustrated by the results for  $\text{Ga}_n^+$  and  $\text{Ga}_{n-1}\text{Al}^+$  with  $n = 30, 31, 32,$  and  $33$  where substantial fluctuations in the size of the peaks for the  $\text{Ga}_n^+$  clusters are mirrored in the results for the  $\text{Ga}_{n-1}\text{Al}^+$  analogs. In all cases reported here the melting temperature of the  $\text{Ga}_{n-1}\text{Al}^+$  analogs are quite similar to those for the pure  $\text{Ga}_n^+$  clusters. This is best illustrated by clusters with  $n = 42, 45,$  and  $46$  where the substantial (200 K) jump in the position of the peak for the  $\text{Ga}_n^+$  clusters is tracked by the peak for the  $\text{Ga}_{n-1}\text{Al}^+$  analogs.

For some clusters such as  $n = 17, 19,$  and  $31$  there is no significant peak in the heat capacities. This may indicate that melting occurs outside the temperature range examined or that melting occurs without a significant latent heat. For the pure gallium clusters, both experiment (ion mobility measurements performed in conjunction with calorimetry measurements)<sup>28</sup> and simulations<sup>29,34</sup> agree on the latter explanation. The simulations suggest that clusters that do not show a well-defined peak in their heat capacities have disordered ground states where there is a relatively broad distribution of coordination numbers, bond lengths, and bond energies. Clusters with more ordered ground states show sharp peaks in their heat capacities. So in a sense, the size of the peak in the heat capacities provides a measure of the degree of order in the solid-like state of the clusters. The fact that the peaks in the heat capacities for the aluminum-containing clusters are very similar to those for the pure gallium analogs suggests that substitution by the aluminum atom does not cause a substantial change in the geometry of the clusters.

The objective of this work was to investigate how substitution by a smaller atom into a gallium cluster would affect the melting temperature. Since the effect in this case appears to be quite modest, we should examine the differences between aluminum and gallium. The room-temperature molar volumes of solid gallium and aluminum are 11.80 and 9.99  $\text{cm}^3$ , respectively. From this we can estimate that the diameter of an aluminum atom is around 5.4% smaller than that of a gallium atom. However, solid bulk gallium does not have one of the simple crystal structures. The most stable phase under normal conditions is orthorhombic and contains gallium dimers. This unusual structure is reflected in the fact that the density increases when gallium melts. Perhaps a more meaningful measure of the relative sizes of gallium and aluminum atoms can be obtained by comparing

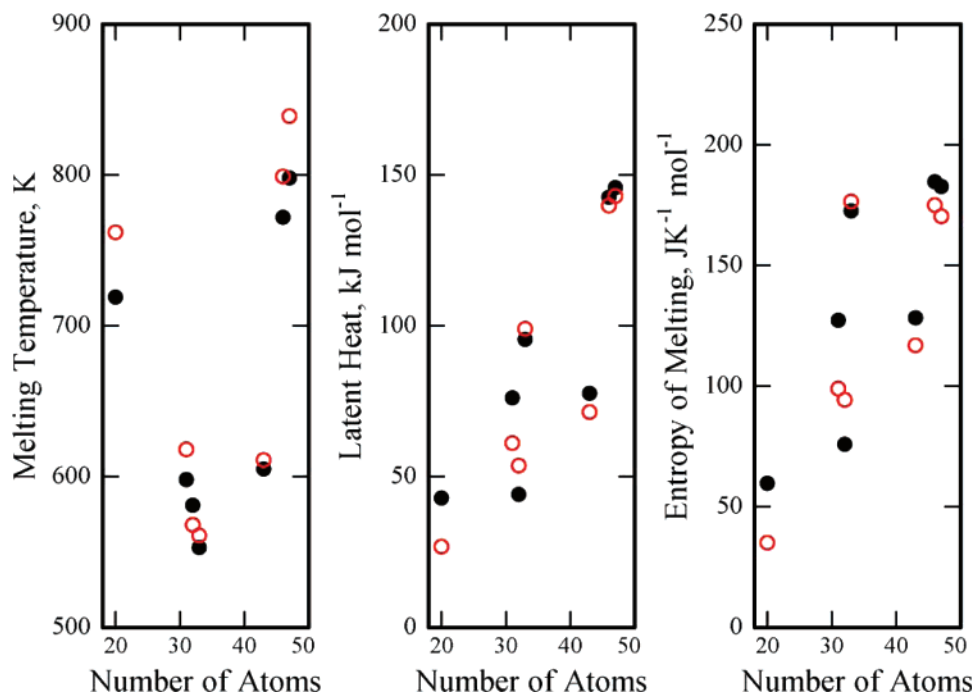


**Figure 3.** Melting temperatures, latent heats, and entropy changes for melting of  $\text{Ga}_n^+$  (filled circles) and  $\text{Ga}_{n-1}\text{Al}^+$  (open circles) plotted against the number of atoms in the cluster. Results are shown for clusters that show a significant heat capacity peak ( $n = 20, 31, 32, 33, 43, 46,$  and  $47$ ).

the densities of the liquid metals. Using the liquid coefficients of expansion to compare the liquid densities at the gallium and aluminum melting points, one finds that the diameter of the aluminum atom is around 3% less than that of the gallium atom. This difference is much smaller than in the cases of Ag/Cu and Ag/Ni core-shell clusters where the different-sized atoms were found (in calculations) to strongly stabilize polyicosahedral geometries.<sup>11</sup> In these cases, the copper and nickel atoms are smaller than the silver atom by 11.5% and 13.8%, respectively.<sup>41</sup> So the small differences between the melting behavior of the  $\text{Ga}_{n-1}\text{Al}^+$  clusters and their pure gallium analogs probably results because the aluminum and gallium atoms have sizes that are not dramatically different. Since gallium is immediately below aluminum in the periodic table, the chemical similarities between these two metals may also contribute.

Although the melting temperatures for the  $\text{Ga}_n^+$  and  $\text{Ga}_{n-1}\text{Al}^+$  clusters are similar, on close inspection there are small shifts (see Figure 3). In most cases where the shifts are significant (i.e.,  $>20$  K) ( $n = 20, 31, 45,$  and  $46$ ) the  $\text{Ga}_{n-1}\text{Al}^+$  analogs have slightly higher melting temperatures than the pure  $\text{Ga}_n^+$  clusters. For  $n = 32$  the shift is in the other direction. The shifts are quite small when compared with the width of the transitions. However, the fact that the majority of the clusters show a shift in the same direction (to higher temperature) when the aluminum atom is substituted makes us more confident that this is a real effect. For the larger  $\text{Ga}_{n-1}\text{Al}^+$  clusters examined here the fraction of aluminum present is close to that found in the bulk eutectic. The bulk eutectic melts at slightly below the melting point of bulk gallium. So it appears that the small shift in the melting temperatures of the clusters is in the opposite direction from that found in the bulk material.

The relationship between the latent heat ( $\Delta H_{\text{fusion}}$ ), the melting temperature ( $T_{\text{melt}}$ ), and the entropy change for melting ( $\Delta S_{\text{fusion}}$ ) is given by

$$\Delta S_{\text{fusion}} = \frac{\Delta H_{\text{fusion}}}{T_{\text{melt}}} \quad (1)$$

Since the melting temperatures and the latent heats for the  $\text{Ga}_{n-1}\text{Al}^+$  clusters and the corresponding  $\text{Ga}_n^+$  clusters are similar, the entropy changes must also be similar. The plot on the right-hand side of Figure 3 shows the entropy changes deduced for the  $\text{Ga}_n^+$  and  $\text{Ga}_{n-1}\text{Al}^+$  clusters from the measured latent heats and melting temperatures using eq 1. The entropy changes for the  $\text{Ga}_{n-1}\text{Al}^+$  clusters are either almost equal to, or slightly less than, the entropy changes for the  $\text{Ga}_n^+$  clusters, with the exception of  $n = 32$ . If the aluminum atom is preferentially located at a particular site in the solid-like cluster but becomes free to occupy any site in the liquid-like cluster there is an additional contribution to the entropy change (due to permutation between the liquid sites). This contribution can be estimated from  $\Delta S_{\text{per}} = R \ln n$  and is around  $24.9\text{--}32.0$  J  $\text{K}^{-1} \text{mol}^{-1}$  for the cluster sizes studied here. The entropy changes determined for the  $\text{Ga}_{n-1}\text{Al}^+$  clusters exceed that for the  $\text{Ga}_n^+$  analogs by an amount approaching  $\Delta S_{\text{per}}$  for only one cluster size,  $n = 32$ . This suggests that the aluminum atom is randomly or nearly randomly arranged between the available sites in the solid-like clusters. Another possible interpretation of the entropy differences is that the aluminum atom is located in a specific site in both the solid-like and liquid-like states (this would also lead to the entropy changes for the  $\text{Ga}_{n-1}\text{Al}^+$  clusters being similar to those for  $\text{Ga}_n^+$ ). A preferential location for the aluminum atom in the liquid-like cluster seems unlikely, but it could occur if the aluminum atom segregates away from the surface since there are only a few internal sites in these clusters.

To further examine this idea we performed some simple calculations. The program Gaussian<sup>42</sup> was used to optimize four structures: (1)  $\text{Ga}_{12}\text{Al}^+$  with icosahedral symmetry and the aluminum atom in the center; (2)  $\text{Ga}_{12}\text{Al}^+$  with an icosahedral geometry and the aluminum atom occupying one of the 12 degenerate surface positions; (3)  $\text{Ga}_{12}\text{Al}^+$  with a slightly distorted icosahedral geometry and the aluminum atom occupying the center site; (4)  $\text{Ga}_{12}\text{Al}^+$  with an icosahedral geometry and the aluminum atom occupying one of the 12 degenerate surface positions. The  $\text{Ga}_{12}\text{Al}^+$  anion is a closed-shell system, and when

**TABLE 1: Calculated Energy Differences between the Optimized Geometries for Icosahedral Ga<sub>12</sub>Al with the Aluminum Inside and Outside for the Anion and Cation Species:  $E(\text{Ga}_{12}\text{Al}^{\pm}/\text{Al Inside}) - E(\text{Ga}_{12}\text{Al}^{\pm}/\text{Al Outside})^a$** 

anion		cation	
HF/6-31G eV	MP2/6-31G eV	HF/6-31G eV	MP2/6-31G eV
2.162	1.881	0.983	1.058

<sup>a</sup> Calculations were done at the HF/6-31G and MP2/6-31G levels.

the aluminum atom is incorporated in the center, the cluster retains icosahedral symmetry. When the aluminum atom is in the shell of the anion, the geometry distorts from icosahedral. The Ga<sub>12</sub>Al<sup>+</sup> cation is not a closed-shell species, and the geometry with the aluminum atom in the center undergoes a Jahn–Teller distortion. For both the anion and the cation the geometries with aluminum on the outside of the cluster were lower in energy than the geometries with aluminum in the center of the cluster, as shown in Table 1. The energy difference is around 1 eV for the anion and around 2 eV for the cation. These results suggest that the most favorable sites for locating the aluminum atom are surface sites on the cluster. In clusters of the size examined in the experiments, most of the atoms are surface atoms, and so a preference for surface sites is consistent with the entropy arguments presented above that the aluminum atom is not strongly localized to a specific site in the Ga<sub>n-1</sub>Al<sup>+</sup> clusters. On the other hand, this behavior differs from that found with the bulk eutectic where it has been reported that the aluminum segregates away from the surface.<sup>36</sup>

## Conclusions

We have examined the melting of Ga<sub>n-1</sub>Al<sup>+</sup> clusters (with  $n = 17, 19, 20, 30-33, 43, 46,$  and  $47$ ) and compared the results to previous calorimetry measurements for Ga<sub>n</sub><sup>+</sup> clusters. Substituting an aluminum atom for a gallium atom causes relatively minor changes in the melting behavior. Large variations in the melting temperatures and latent heats observed for Ga<sub>n</sub><sup>+</sup> clusters are mirrored by the Ga<sub>n-1</sub>Al<sup>+</sup> clusters. In many cases, the Ga<sub>n-1</sub>Al<sup>+</sup> clusters appear to have slightly higher melting temperatures, unlike the bulk eutectic which has a lower melting temperature than pure gallium. The entropy changes for melting of the Ga<sub>n-1</sub>Al<sup>+</sup> clusters are in most cases similar to, or slightly less than, those for the pure Ga<sub>n</sub><sup>+</sup> clusters. This suggests that the aluminum atom is not localized to a particular site in the solid-like cluster. From the experimental results and calculations, it appears that surface sites are the preferred location for the aluminum atom in the Ga<sub>n-1</sub>Al<sup>+</sup> clusters.

**Acknowledgment.** We gratefully acknowledge the support of the National Science Foundation. We thank Krishnan Raghavachari and Glen Ferguson for help with the calculations.

## References and Notes

- Beck, S. M. Mixed Metal–Silicon Clusters Formed by Chemical Reaction in a Supersonic Molecular Beam: Implications for Reactions at the Metal Silicon Interface. *J. Chem. Phys.* **1989**, *90*, 6306–6312.
- Jackson, K.; Nellermoe, B. Zr@Si<sub>20</sub>: A Strongly Bound Si Endohedral System. *Chem. Phys. Lett.* **1996**, *254*, 249–256.
- Jellinek, J.; Krissinel, E. B. Ni<sub>n</sub>Al<sub>m</sub> Alloy Clusters: Analysis of Structural Forms and Their Energy Ordering. *Chem. Phys. Lett.* **1996**, *258*, 283–292.
- Thomas, O. C.; Zheng, W.; Bowen, K. H. Magic Numbers in Copper-Doped Aluminum Cluster Anions. *J. Chem. Phys.* **2001**, *114*, 5514–5519.
- Hiura, H.; Miyazaki, T.; Kanayama, T. Formation of Metal-Encapsulating Si Cage Structures. *Phys. Rev. Lett.* **2001**, *86*, 1733–1736.

- Khanna, S. N.; Ashman, C.; Rao, B. K.; Jena, P. Geometry, Electronic Structure, and Energetics of Copper-Doped Aluminum Clusters. *J. Chem. Phys.* **2001**, *114*, 9792–9796.
- Rexer, E. F.; Jellinek, J.; Krissinel, E. B.; Parks, E. K.; Riley, S. J. Theoretical and Experimental Studies of the Structures of 12-, 13-, and 14-Atom Bimetallic Nickel/Aluminum Clusters. *J. Chem. Phys.* **2002**, *117*, 82–94.
- Gaudry, M.; Cottancin, E.; Pellarin, M.; Lermé, J.; Arnaud, L.; Huntzinger, J. R.; Vialle, J. L.; Broyer, M.; Rousset, J. L.; Treilleux, M.; Mélinon, P. Size and Composition Dependence in the Optical Properties of Mixed (Transition Metal/Noble Metal) Embedded Clusters. *Phys. Rev. B* **2003**, *67*, 155409.
- Joshi, K.; Kanhere, D. G. Finite Temperature Behavior of Impurity Doped Lithium Cluster, Li<sub>6</sub>Sn. *J. Chem. Phys.* **2003**, *119*, 12301–12307.
- Kumar, V. Novel Metal-Encapsulated Caged Clusters of Silicon and Germanium. *Eur. Phys. J. D* **2003**, *24*, 227–232.
- Rossi, G.; Rapallo, A.; Mottet, C.; Fortunelli, A.; Baletto, F.; Ferrando, R. Magic Polycosahedral Core–Shell Clusters. *Phys. Rev. Lett.* **2004**, *93*, 105503.
- Breaux, G. A.; Hillman, D. A.; Neal, C. M.; Jarrold, M. F. Stable Copper–Tin Cluster Compositions from High Temperature Annealing. *J. Phys. Chem. A* **2005**, *109*, 755–759.
- Aguado, A.; López, J. M. Structural and Thermal Behavior of Compact Core–Shell Nanoparticles: Core Instabilities and Dynamic Contributions to Surface Thermal Stability. *Phys. Rev. B* **2005**, *72*, 205420.
- Rapallo, Q. A.; Rossi, G.; Ferrando, R.; Fortunelli, A.; Curley, B. C.; Lloyd, L. D.; Tarbuck, G. M.; Johnston, R. L. Global Optimization of Bimetallic Cluster Structures. I. Size Mismatched Ag–Cu, Ag–Ni, and Au–Cu Systems. *J. Chem. Phys.* **2005**, *122*, 194308.
- Rossi, G.; Ferrando, R.; Rapallo, A.; Fortunelli, A.; Curley, B. C.; Lloyd, L. D.; Johnston, R. L. Global Optimization of Bimetallic Cluster Structures. II. Size-Matched Ag–Pd, Ag–Au, and Pd–Pt Systems. *J. Chem. Phys.* **2005**, *122*, 194309.
- Michaelian, K.; Garzon, I. L. Thermodynamic Properties of Au<sub>n</sub>–Ag<sub>n</sub> Bimetallic Clusters Through the Evolutive Ensemble. *Eur. Phys. J. D* **2005**, *34*, 183–186.
- Schmidt, M.; Kusche, R.; Kronmüller, W.; von Issendorff, B.; Haberland, H. Experimental Determination of the Melting Point and Heat Capacity for a Free Cluster of 139 Sodium Atoms. *Phys. Rev. Lett.* **1997**, *79*, 99–102.
- Schmidt, M.; Kusche, R.; von Issendorff, B.; Haberland, H. Irregular Variations in the Melting Point of Size-Selected Atomic Clusters. *Nature* **1998**, *393*, 238–240.
- Kusche, R.; Hippler, T.; Schmidt, M.; von Issendorff, B.; Haberland, H. Melting of Free Sodium Clusters. *Eur. Phys. J. D* **1999**, *9*, 1–4.
- Schmidt, M.; Kusche, R.; Hippler, T.; Donges, J.; Kronmüller, W.; von Issendorff, B.; Haberland, H. Negative Heat Capacity for a Cluster of 147 Sodium Atoms. *Phys. Rev. Lett.* **2001**, *86*, 1191–1194.
- Schmidt, M.; Haberland, H. Phase Transitions in Clusters. *C. R. Phys.* **2002**, *3*, 327–340.
- Schmidt, M.; Donges, J.; Hippler, T.; Haberland, H. Influence of Energy and Entropy on the Melting of Sodium Clusters. *Phys. Rev. Lett.* **2003**, *90*, 103401.
- Haberland, H.; Hippler, T.; Donges, J.; Kostko, O.; Schmidt, M.; von Issendorff, B. Melting of Sodium Clusters: Where Do the Magic Numbers Come From? *Phys. Rev. Lett.* **2005**, *94*, 035701.
- Shvartsburg, A. A.; Jarrold, M. F. Solid Clusters above the Bulk Melting Point. *Phys. Rev. Lett.* **2000**, *85*, 2530–2532.
- Breaux, G. A.; Neal, C. M.; Cao, B.; Jarrold, M. F. Tin Clusters that Do Not Melt: Calorimetry Measurements up to 650 K. *Phys. Rev. B* **2005**, *71*, 073410.
- Breaux, G. A.; Benirschke, R. C.; Sugai, T.; Kinnear, B. S.; Jarrold, M. F. Hot and Solid Gallium Clusters: Too Small to Melt. *Phys. Rev. Lett.* **2003**, *91*, 215508.
- Breaux, G. A.; Hillman, D. A.; Neal, C. M.; Benirschke, R. C.; Jarrold, M. F. Gallium Cluster “Magic Melters”. *J. Am. Chem. Soc.* **2004**, *126*, 8628–8629.
- Breaux, G. A.; Cao, B.; Jarrold, M. F. Second-Order Phase Transitions in Amorphous Gallium Clusters. *J. Phys. Chem.* **2005**, *109*, 16575–16578.
- Krishnamurthy, S.; Chacko, S.; Kanhere, D. G.; Breaux, G. A.; Neal, C. M.; Jarrold, M. F. Size-Sensitive Melting Characteristics of Gallium Clusters: Comparison of Experiment and Theory for Ga<sub>17</sub><sup>+</sup> and Ga<sub>20</sub><sup>+</sup>. *Phys. Rev. B* **2006**, *73*, 045406.
- Breaux, G. A.; Benirschke, R. C.; Jarrold, M. F. Melting, Freezing, Sublimation, and Phase Coexistence in Sodium Chloride Nanocrystals. *J. Chem. Phys.* **2004**, *121*, 6502–6507.
- Breaux, G. A.; Neal, C. M.; Cao, B.; Jarrold, M. F. Melting, Premelting, and Structural Transitions in Size-Selected Aluminum Clusters with around 55 Atoms. *Phys. Rev. Lett.* **2005**, *94*, 173401.
- Neal, C. M.; Starace, A. K.; Jarrold, M. F. Ion Calorimetry: Using Mass Spectrometry to Measure Melting Points. *J. Am. Soc. Mass Spectrom.* **2007**, *18*, 74–81.

- (33) Pawlow, P. Über die Abhängigkeit des Schmelzpunktes von der Oberflächenenergie eines Festen Körpers. *Z. Phys. Chem.* **1909**, *65*, 1–35.
- (34) Joshi, K.; Krishnamurty, S.; Kanhere, D. G. “Magic Melters” Have Geometrical Origin. *Phys. Rev. Lett.* **2006**, *96*, 135703.
- (35) Sun, D. Y.; Gong, X. G. Structural Properties and Glass Transition in  $Al_n$  Clusters. *Phys. Rev. B* **1998**, *57*, 4730–4735.
- (36) Lill, Th.; Calaway, W. F.; Pellin, M. J. Cluster Emission During Sputtering of Liquid Gallium–Aluminum Alloy. *J. Chem. Phys.* **1995**, *78*, 505–509.
- (37) Neal, C. M.; Breaux, G. A.; Cao, B.; Starace, A. K.; Jarrold, M. F. Improved Signal Stability from a Laser Vaporization Source with a Liquid Metal Target. *Rev. Sci. Instrum.* **2007**, *78*, 075108.
- (38) Jarrold, M. F.; Honea, E. C. Annealing of Silicon Clusters. *J. Am. Chem. Soc.* **1992**, *114*, 459–464.
- (39) Jarrold, M. F.; Honea, E. C. Dissociation of Large Silicon Clusters: The Approach to Bulk Behavior. *J. Phys. Chem.* **1991**, *95*, 9181–9185.
- (40) Bohr, J. Quantum Mode Phonon Forces between Chain Molecules. *Int. J. Quantum Chem.* **2001**, *84*, 249–252.
- (41) Using the bulk densities. Copper, nickel, and silver all have fcc crystal structures.
- (42) Frisch, M. J.; Trucks, G. W.; Schlegel, H. B.; Scuseria, G. E.; Robb, M. A.; Cheeseman, J. R.; Montgomery, J. A., Jr.; Vreven, T.; Kudin, K. N.; Burant, J. C.; Millam, J. M.; Iyengar, S. S.; Tomasi, J.; Barone, V.; Mennucci, B.; Cossi, M.; Scalmani, G.; Rega, N.; Petersson, G. A.; Nakatsuji, H.; Hada, M.; Ehara, M.; Toyota, K.; Fukuda, R.; Hasegawa, J.; Ishida, M.; Nakajima, T.; Honda, Y.; Kitao, O.; Nakai, H.; Klene, M.; Li, X.; Knox, J. E.; Hratchian, H. P.; Cross, J. B.; Adamo, C.; Jaramillo, J.; Gomperts, R.; Stratmann, R. E.; Yazyev, O.; Austin, A. J.; Cammi, R.; Pomelli, C.; Ochterski, J. W.; Ayala, P. Y.; Morokuma, K.; Voth, G. A.; Salvador, P.; Dannenberg, J. J.; Zakrzewski, V. G.; Dapprich, S.; Daniels, A. D.; Strain, M. C.; Farkas, O.; Malick, D. K.; Rabuck, A. D.; Raghavachari, K.; Foresman, J. B.; Ortiz, J. V.; Cui, Q.; Baboul, A. G.; Clifford, S.; Cioslowski, J.; Stefanov, B. B.; Liu, G.; Liashenko, A.; Piskorz, P.; Komaromi, I.; Martin, R. L.; Fox, D. J.; Keith, T.; Al-Laham, M. A.; Peng, C. Y.; Nanayakkara, A.; Challacombe, M.; Gill, P. M. W.; Johnson, B.; Chen, W.; Wong, M. W.; Gonzalez, C.; Pople, J. A. *Gaussian 03*, revision B.05; Gaussian, Inc.: Pittsburgh, PA, 2003.